LIMNOLOGY
and
OCEANOGRAPHY: METHODS

ASLO

Limnol. Oceanogr.: Methods 23, 2025, 326–335

doi: 10.1002/lom3.10683

EVALUATIONS OF EXISTING METHODS

Particulate inorganic carbon in the ocean: Evaluation of discrete sampling protocols

Catherine Mitchell [1]*, **Jelena Godrijan** [1,2]*

[1]Bigelow Laboratory for Ocean Sciences, East Boothbay, Maine, USA; [2]Division for Marine and Environmental Research, Ruđer Bošković Institute, Zagreb, Croatia

Abstract

This study evaluates the impact of sampling protocols on the measurement of particulate inorganic carbon (PIC) in ocean waters, an essential component for understanding the global carbon cycle and climate regulation. The study compares four protocols for estimating PIC in discrete water column samples, focusing on the effects of filter pore size (0.4 vs. 0.8 μm) and rinsing agents (pH-adjusted MilliQ water with NH_4OH vs. potassium tetraborate buffer). Five coccolithophore strains were selected to represent variations in PIC content resulting from species-specific differences in coccolith mass, coccolith number per cell, and life cycle phase. Discrete samples were analyzed using inductively coupled plasma mass spectrometry. Statistical analyses show no significant differences in PIC concentrations between protocols, filter types, or rinsing agents, confirming the robustness and precision of the measurement method. In addition, the non-calcifying strain provided insights into the measurement uncertainty and enabled us to quantify the precision of the sampling method. These results suggest that researchers can use any tested protocol without compromising data quality. This will improve the reliability and comparability of PIC measurements and contribute to a more precise understanding of ocean carbon dynamics and climate regulation.

Particulate inorganic carbon (PIC) is one of the major reservoirs of carbon in the ocean, is related to atmospheric CO_2, and plays a crucial role in global biogeochemical cycles and carbon sequestration (Klaas and Archer 2002; Mitchell et al. 2017). By influencing the alkalinity of the ocean and the ocean's ability to absorb atmospheric CO_2, PIC significantly affects global climate regulation (Millero 2007). While PIC formation through calcification reduces alkalinity, its net effect on carbon cycling depends on whether it is exported to depth and removed from surface waters or dissolves at shallower depths, which can counteract its initial impact. This underscores the importance of precise estimates of global PIC distribution and its temporal variability for understanding ocean carbon dynamics.

In the ocean, PIC is present in the form of a mineral calcium carbonate ($CaCO_3$), formed through a biologically facilitated process known as calcification (Milliman 1993; Monteiro et al. 2016). While several groups of organisms produce $CaCO_3$, coccolithophores dominate the living pelagic $CaCO_3$ stock and play a major role in global carbonate cycling. Recent estimates suggest that coccolithophores contribute 26–52% of global $CaCO_3$ export fluxes, with the remainder primarily attributed to foraminifera and pteropods, though their relative contributions vary regionally and with depth (Knecht et al. 2023; Neukermans et al. 2023). In surface waters, coccolithophores are estimated to produce up to 90% of suspended $CaCO_3$, as indicated by in situ and satellite-based studies (Ziveri et al. 2023) highlighting their key role in the upper ocean carbonate cycle.

Coccolithophores are unicellular haptophyte algae that produce coccoliths, calcite plates that adorn their cells (Billard

*Correspondence: cmitchell@bigelow.org, jelena.godrijan@irb.hr

Associate editor: Xiao Hua Wang

Data Availability Statement: The data that support the findings of this study are openly available in ZENODO at http://doi.org/10.5281/zenodo.14939398.

and Inouye 2004). In these organisms, the highly regulated process of calcification—or coccolith formation—takes place within the cell (Ben-Joseph et al. 2023; Brownlee et al. 2021). Despite their minute size (a few micrometers), coccoliths display considerable species-specific morphological diversity, with about 280 species-specific morphotypes identified (Frada et al. 2019; Young et al. 2003). They are mainly categorized into two types corresponding to their life cycle phases: (1) heterococcoliths, intricately shaped single calcite crystals that adorn diploid cells possessing two sets of chromosomes, and (2) holococcoliths, which consist of numerous small rhombohedral calcite crystals forming complex structures on haploid cells with a single set of chromosomes (Henriksen et al. 2004; Langer et al. 2021).

Estimates of PIC in the ocean are typically obtained from discrete water samples (Balch et al. 2000; Poulton et al. 2006), sediment traps (Honjo et al. 2000), optical proxies (Balch and Fabry 2008; Balch et al. 2014), and remote sensing (Balch and Mitchell 2023; Hopkins and Balch 2018), each with distinct advantages and limitations. Discrete samples provide detailed, depth-specific data, but are limited to specific points in time and space. Sediment traps provide temporal and depth-related insights but primarily collect sinking material from depths significantly deeper than where PIC is produced. As a result, they integrate data over larger areas and time scales, potentially masking short-term changes and surface production dynamics. Optical proxies provide high spatial resolution by enabling continuous, flow-through PIC measurements from ships' underway systems, offering valuable insights into surface PIC distributions. Their primary limitation has traditionally been their restriction to surface observations, but recent advancements in birefringence-based sensors have expanded their applicability to deeper water column measurements, particularly when deployed on autonomous platforms and profiling systems (Bishop et al. 2022). Remote sensing allows large-scale, continuous monitoring, but does not provide depth resolution. In this paper, we focus on discrete sampling due to its detailed resolution and its role in validating and calibrating optical proxy and remote sensing methods.

Remote sensing of PIC relies on the strong light scattering properties of calcite, the $CaCO_3$ mineral in coccoliths (Balch et al. 1999; Balch et al. 1991). This scattering produces a distinct optical signal that can be detected by satellites (Holligan et al. 1993). Instruments such as the sea-viewing wide field-of-view sensor and the moderate resolution imaging spectroradiometer have been used to detect this signal and estimate surface PIC concentrations, enabling large-scale monitoring of PIC in the ocean (Balch et al. 2005; Gordon et al. 2001; Moore et al. 2012). There are several PIC algorithms, which combine ocean color (water-leaving radiance or remote sensing reflectance) with the calcite-specific backscattering coefficient from coccolithophores, providing a measure of coccolithophore PIC concentration (Balch and Mitchell 2023). With the launch of the new satellite platform PACE (Plankton, Aerosol, Cloud, ocean Ecosystem) in early 2024 (Gorman et al. 2019), more degrees of freedom for more detailed quantification of PIC will be possible, allowing new algorithms to be developed. An essential measurement for both algorithm development and validation is PIC concentration from discrete samples (Mitchell et al. 2017). Thus, the main purpose of this article is to evaluate the currently used sampling protocols for discrete PIC samples.

When estimating PIC in discrete water column samples, two primary methods are commonly used. The first is the carbon subtraction method, where PIC is indirectly estimated by subtracting particulate organic carbon from total particulate carbon. In this approach, samples are filtered using precombusted glass fiber filters, and total particulate carbon and particulate organic carbon are measured separately using a CHN analyzer; the particulate organic carbon filter is analyzed after carbonate removal by acidification (Van Iperen and Helder 1985). Particulate inorganic carbon is calculated as the difference between total particulate carbon and particulate organic carbon. This method can lead to significant errors due to the separate measurements, error propagation, and the compounding of the individual measurement errors, as also noted by Daniels et al. (2018) in the context of calcification rate measurements.

An alternative method for estimating the standing stock of PIC involves chemically analyzing particulate calcium, assuming that all particulate calcium is in the form of calcium carbonate (Fernández et al. 1993). In this approach, seawater samples are filtered, and the particulate calcium is extracted by acid leaching of the filter. Multiple techniques are available for measuring the extracted calcium (Balch and Fabry 2008), as well as inductively coupled plasma mass spectrometry (ICP-MS) (Platzner et al. 2008) and optical emission spectroscopy (Balch and Drapeau 2003). The ICP-MS offers greater sensitivity and lower detection limits compared to inductively coupled plasma optical emission spectroscopy, making it particularly suitable for detecting trace levels of PIC in oceanic samples. This direct measurement is more precise and reliable for assessing PIC in the ocean, especially at low concentrations, since it avoids an additional subtraction step. Since this method assumes that all particulate calcium is present as $CaCO_3$, the background concentration of calcium in seawater ($\sim$10 mM [mmol L^{-1}]) poses a challenge. To precisely detect nanogram quantities of particulate calcium, the dissolved Ca^{2+} in seawater must be completely rinsed away (Balch and Fabry 2008). This is usually achieved by thoroughly rinsing the filters with a rinsing agent to remove calcium salts such as $CaCl_2$ (Fernández et al. 1993). However, the research groups using this sensitive PIC estimation method use different sampling protocols with various filters and rinsing agents. In view of our planned validation efforts, we aim to evaluate the differences between these protocols.

With our assessment, we investigated how variations in the PIC protocol, in particular the pore size of the filters and the choice of rinsing agent, could affect the PIC measurement results. We focused on two filter pore sizes: 0.4 and 0.8 μm, even though some researchers also used the 0.2-μm pore size (Daniels et al. 2012; Fernández et al. 1993). It was expected that the 0.4-μm filters would retain all coccolith particles, based on published sizes indicating that coccoliths are larger than 0.4 μm (Balch et al. 2000; Winter and Siesser 1994). In contrast, the 0.8-μm filters were selected under the assumption that they would allow for faster filtration times without compromising the precision of the PIC measurements (Daniels et al. 2012). We also investigated the effects of different rinsing agents on the precision of the PIC measurements. We tested two rinsing agents: pH-adjusted with trace ammonia MilliQ water solution (pH ~ 10–11) (Daniels et al. 2012; Mayers et al. 2019), and 0.02-M potassium tetraborate buffer (Balch et al. 2000; Poulton et al. 2006). We wanted to find out whether one of the two agents offers advantages in stabilizing the particulate calcium during the rinsing process.

By testing different filter pore sizes and rinsing agents, we aimed to determine their effects on PIC results and identify the most effective combination for precise and efficient PIC sampling. This would provide valuable guidance on best practices for standardizing sampling procedures.

Materials and procedures

Materials

For our experiment, we selected five coccolithophore strains with diverse coccolith morphologies, allowing us to assess potential sampling biases related to calcite structure. We used three strains of *Calcidiscus leptoporus*: (1) diploid strain (RCC1164) that produces large, heavily calcified placolith coccoliths with prominent central area structures, (2) calcifying haploid strain (*C. leptoporus* subsp. *leptoporus* HOL, RCC1151) that forms holococcoliths composed of numerous rhombohedral calcite crystals arranged in a uniform, plate-like structure, and (3) a non-calcifying haploid (RCC1129). Additionally, we included a diploid *Umbilicosphaera foliosa* strain (RCC1472), which produces placolith coccoliths with an open central area, and a haploid strain of *Syracosphaera pulchra* (*S. pulchra* HOL oblonga type, MIR02), which forms dome-shaped holococcoliths composed of a continuous layer of crystallites arranged in a hexagonal array. Strains marked with RCC were obtained from the Roscoff Culture Collection, while *S. pulchra* HOL was isolated from the Adriatic Sea off the island of Zlarin on June 9, 2023 by Jelena Godrijan (see Table 1). This selection ensured a diverse representation of coccolith morphologies, including placoliths with varying degrees of calcification and holococcoliths composed of delicate, rhombohedral crystallites, allowing us to evaluate potential sampling biases related to structural differences in calcite organization.

Prior to the experiment, the culture strains were maintained in 50-mL vented tissue culture flasks (Techno Plastic Products) within a thermostatic chamber (Inkolab) set at 17°C under a 12 : 12 h light/dark cycle with illumination of approximately 68 μmol photons m^{-2} s^{-1} from a white LED light source. The strains were grown in batch cultures using K/4 medium prepared with aged Adriatic seawater at salinity 38.6 (S38.6), which was adjusted to salinity 35 (S35) with MilliQ water for the RCC cultures. The S38 K/4 medium was used exclusively for cultivating the MIR02 strain. Growth of each strain was monitored by measuring cell concentrations. Samples for cell counts were fixed with glutaraldehyde at a final concentration of 5% (Sigma-Aldrich) for 30 min before being counted in glass Sedgewick Rafter counting chambers (Graticules Optics Ltd) using an AE2000 inverted light microscope (MoticEurope, S.L.U.).

For the experimental testing, we used 0.4 and 0.8 μm polycarbonate filters (Isopore PC Membrane, Merck Millipore Ltd). Polycarbonate filters help reduce blank values compared to filters that retain more residual seawater, such as glass fiber filters, which can introduce background calcium contamination (Balch et al. 2000; Poulton et al. 2006). The pH-adjusted MilliQ water was prepared by adding 180 μL of 25% ammonia (NH_4OH) solution for analysis EMSURE® ISO, Reag. Ph Eur (Supelco) to 1 L of MilliQ water, resulting in a pH range of 9–10 and optimized for rinsing efficiency. The potassium tetraborate buffer was prepared by dissolving 3.06 g of 99.5% potassium tetraborate tetrahydrate ($K_2B_4O_7$) ReagentPlus®, ≥99.5% (Sigma-Aldrich) in 500 mL of MilliQ water.

Procedures

Experimental setup and sample collection

To determine the optimal combination of filter pore size and rinsing agent for precise and efficient PIC sampling, we prepared 200 mL of each culture strain by adding cells from

Table 1. List of strains used in the experiment.

Code	Strain	Species	Ploidy	Coccolith size	Coccolith type	S
C. leptoporus 2N/HET	RCC1164	*Calcidiscus leptoporus*	Diploid	5–8 μm	Heterococcolith	S35
C. leptoporus N/HOL	RCC1151	*Calcidiscus leptoporus*	Haploid	1.6–2.4 μm	Holococcolith	S35
C. leptoporus N/non-c	RCC1129	*Calcidiscus leptoporus*	Haploid	-	Non-calcifying	S35
U. foliosa 2N/HET	RCC1472	*Umbilicosphaera foliosa*	Diploid	4.5–7 μm	Heterococcolith	S35
S. pulchra N/HOL	MIR02	*Syracosphaera pulchra*	Haploid	1.8–2.8 μm	Holococcolith	S38.6

S, salinity.

cultures in their exponential growth phase into 300-mL tissue culture flasks (Techno Plastic Products). We filtered 15 mL of each prepared culture strain in triplicate for each PIC protocol (0.4 μm and NH_4OH, 0.4 μm and $K_2B_4O_7$, 0.8 μm and NH_4OH, and 0.8 μm and $K_2B_4O_7$). To minimize variability within each culture strain, samples were taken from the same homogenized culture flask, ensuring consistent distribution across replicates. This approach ensures that within-strain comparisons of PIC across protocols are robust and independent of cell abundance. A flask containing pure S35 K/4 medium was used as a blank, and 15 mL of blank triplicate samples were collected for all four PIC protocols. We rinsed the filters with a squirt of rinsing agent (an approximate volume of 2–3 mL), placed the filters in trace metal-free 15-mL sterile centrifuge Falcon® tubes (Corning) and dried them overnight at 50°C. A total of 72 samples were taken ([5 species + blank] × 4 protocols × 3 replicates).

Sample processing

For the determination of Ca and Na, our samples were processed by the ICP-MS Facility at the Climate Change Institute, University of Maine. To extract the samples from the filters, 5 mL of ultraclean 5% nitric acid suitable for Ultra Trace Elemental Analysis was added to each tube. The tubes were then capped, shaken to ensure the filters were fully immersed in the acid, and left to stand for approximately 24 h (overnight). Samples were then transferred to a polypropylene 4-mL vials that have been acid cleaned. Standards were mixed from monoelemental solutions in ultraclean 5% nitric acid, and all standards contained 1 mg L^{-1} K (which was not analyzed). All samples were analyzed using a Thermo Element XR HR-ICP-MS (Thermo Fisher Scientific) and measured in medium resolution. To assess instrument stability and reproducibility, a standard was analyzed approximately every 10–20 samples, a certified reference material was used once per run to verify the calibration, and a blank was included within each calibration curve, with no further blank subtraction performed. The detection limits were 2.5 μg L^{-1} for Ca and 4.0 μg L^{-1} for Na.

Post-analysis corrections

While the purpose of the filter rinse is to remove any calcium-based salts, the rinse step is often incomplete, and some salts remain in the filter residual. Therefore, it is necessary to perform a seawater correction. In seawater of reference salinity (S35) for the standard ocean at 25°C and 101,325 Pa, the relative compositions of the major components calcium (Ca) and sodium (Na) are 412 mg L^{-1} for Ca and 10,781 mg L^{-1} for Na (Millero 2013). The relative composition of salt in seawater remains nearly constant, hence by using the weight fraction, we were able to calculate the relative compositions of Ca and Na at salinity 38.6 (S38.6) for the Adriatic samples, which are 454 mg L^{-1} for Ca and 11,890 mg L^{-1} for Na. Thus, the seawater corrected Ca concentration, Ca_{swc}, was determined as follows:

$$\mathrm{Ca_{swc}} = \mathrm{Ca_{raw}} - \mathrm{Na_{raw}} \frac{\mathrm{Ca_{salt}}}{\mathrm{Na_{salt}}}$$

where the raw in subscript indicates the Ca and Na concentrations as measured by the ICP-MS technique, and the salt in subscript indicates the Ca and Na concentrations in seawater due to salt (in mg L^{-1}).

For determining Ca and Na using the ICP-MS, the residual on the filter was extracted in 5 mL of nitric acid, whereas, the volume of culture originally filtered was 15 mL. Therefore, a volume correction was performed, resulting in Ca concentration in μg L^{-1}, Ca (μg L^{-1}):

$$\mathrm{Ca}\left(\mu\mathrm{g\,L^{-1}}\right) = \mathrm{Ca_{swc}} \frac{V_{\mathrm{ext}}}{V_{\mathrm{filt}}}$$

where V_{ext} is the volume used to extract the filter residual and V_{filt} is the volume of culture originally filtered.

The seawater and volume-corrected Ca concentration values were then converted to molar concentrations. The molar concentration of PIC is equivalent to the molar Ca concentration (as PIC is $CaCO_3$, i.e., 1 mol of Ca and 1 mol of C), thus:

$$\mathrm{PIC}\left(\mathrm{mmol\,m^{-3}}\right) = \mathrm{Ca}\left(\mathrm{mmol\,m^{-3}}\right) = \frac{\mathrm{Ca}\left(\mu\mathrm{g\,L^{-1}}\right)}{40}$$

The PIC molar concentration can be converted back to a mass concentration:

$$\mathrm{PIC}\left(\mu\mathrm{g\,L^{-1}}\right) = \mathrm{PIC}\left(\mathrm{mmol\,m^{-3}}\right) \times 12$$

The final post-analysis step was to perform a blank correction. For each protocol, the mean blank PIC was calculated. For each protocol, the appropriate mean blank PIC values were then subtracted from the PIC concentrations for each sample replicate. The blank PIC values are reported in Table 2, with Fig. 1 showing the blank PIC relative to the PIC concentrations of all cultures. Across all four protocols, the median

Table 2. Particulate inorganic carbon (PIC) blank values across cultures, for each treatment.

Treatment	Mean PIC blank (μg L^{-1})	Mean PIC blank (mmol m^{-3})	Median PIC blank (%)
0.4 μm and NH_4OH	1.42	0.12	9
0.4 μm and $K_2B_4O_7$	1.66	0.14	12
0.8 μm and NH_4OH	2.91	0.24	13
0.8 μm and $K_2B_4O_7$	2.13	0.18	13

blank PIC is 9–13% of the culture PIC concentrations. However, it is worth noting that for the non-calcifying haploid strain *C. leptoporus* N/non-c, the PIC values are similar to the blank values; thus, the percentage is much larger (>100%).

Assessment

In our experiments, we examined how different sampling protocols influenced PIC concentrations in five coccolithophore strains (Fig. 2; Table 3). Importantly, this study focuses on bulk PIC concentrations across protocols, not PIC per cell between cultures, so variations in cell numbers do not affect our comparisons. Samples from the culture of the diploid strain *C. leptoporus* 2N/HET had an average PIC concentration of 98.23 $\mu g\ L^{-1}$ (8.19 $mmol\ m^{-3}$), while those from the diploid strain *U. foliosa* 2N/HET had an average concentration of 19.65 $\mu g\ L^{-1}$ (1.64 $mmol\ m^{-3}$). Among the haploid strains, samples from the culture of *S. pulchra* N/HOL had an average PIC concentration of 3.48 $\mu g\ L^{-1}$ (1.27 $mmol\ m^{-3}$), and *C. leptoporus* N/HOL had 11.20 $\mu g\ L^{-1}$ (0.93 $mmol\ m^{-3}$). Samples from the culture of the non-calcifying haploid strain *C. leptoporus* N/non-c showed negligible PIC concentrations, averaging 0.29 $\mu g\ L^{-1}$ (0.02 $mmol\ m^{-3}$).

Protocol assessment

The main question we asked was whether the different protocols, in particular, the two pore sizes of the filters and the two different rinsing agents, led to different PIC concentrations. To assess this, we determined if there was a statistically significant difference between the median PIC concentrations for each of the protocols using a nonparametric test that does not assume normality in the data and is less sensitive to outliers. We performed a Kruskal–Wallis test between the four protocols (all culture strains together) and found that the p value was greater than 0.05, meaning that the protocols did not differ significantly (statistic = 0.824, $p = 0.844$). We also investigated how different filter types and rinsing agents affect the PIC measurements. We wanted to determine whether there was an effect due to the filter type (independently from the rinse type), the rinse type (independently from the filter type), and/or whether there was an interaction effect between filter type and rinse type, that is, whether the effect of filter type on PIC depended on the rinse agent used. We performed an aligned rank transform (a non-parametric test that allows for interaction effects to be tested) on all the culture strains and found that the p values were greater than 0.05 for all combinations of rinse and filter type. Therefore, neither the filter type nor the rinsing agent nor their interaction had a significant effect on the PIC.

These statistical analyses collectively suggest that neither the sampling protocol nor its components (filter pore size and rinsing agent) significantly affect the PIC concentrations measured. The lack of significant differences across protocols implies that the method is robust and that any of the tested protocols can be reliably used for precise and efficient PIC sampling.

Uncertainty assessment

The *C. leptoporus* N/non-c culture strain served as a control to assess the overall uncertainty of our PIC measurement method, as the expected PIC concentration in this case should

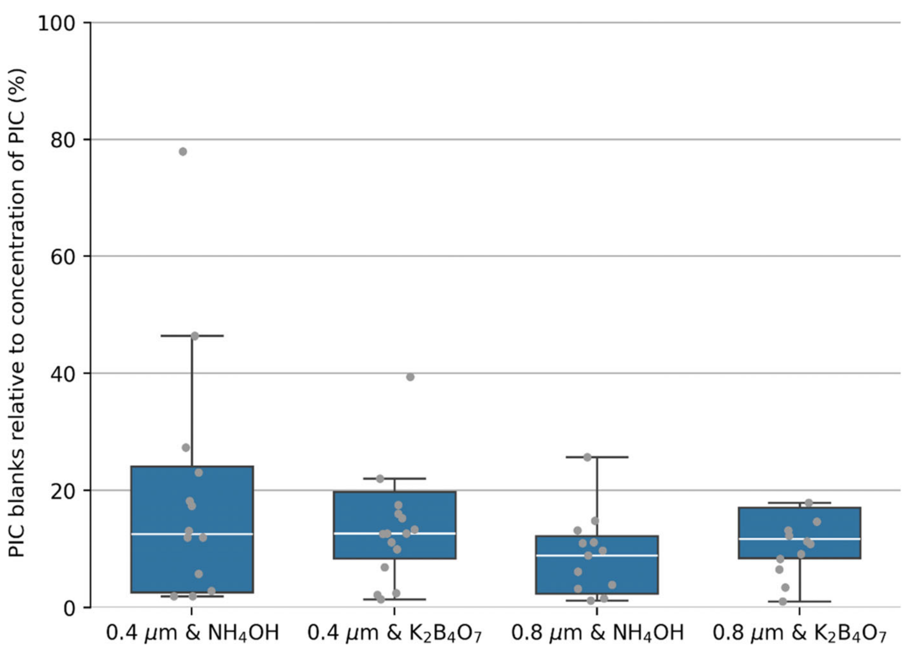

Fig. 1. Boxplot showing the percentage of PIC blank values relative to the measured PIC concentration for different filter pore sizes and rinsing agents. Each dot represents an individual replicate, the solid white line indicates the median, and the box represents the interquartile range (IQR). Whiskers extend to 1.5 times the IQR, with outliers shown as individual points beyond this range. Dots representing blank values of the non-calcifying strain are not presented in this figure as they fall outside the scale.

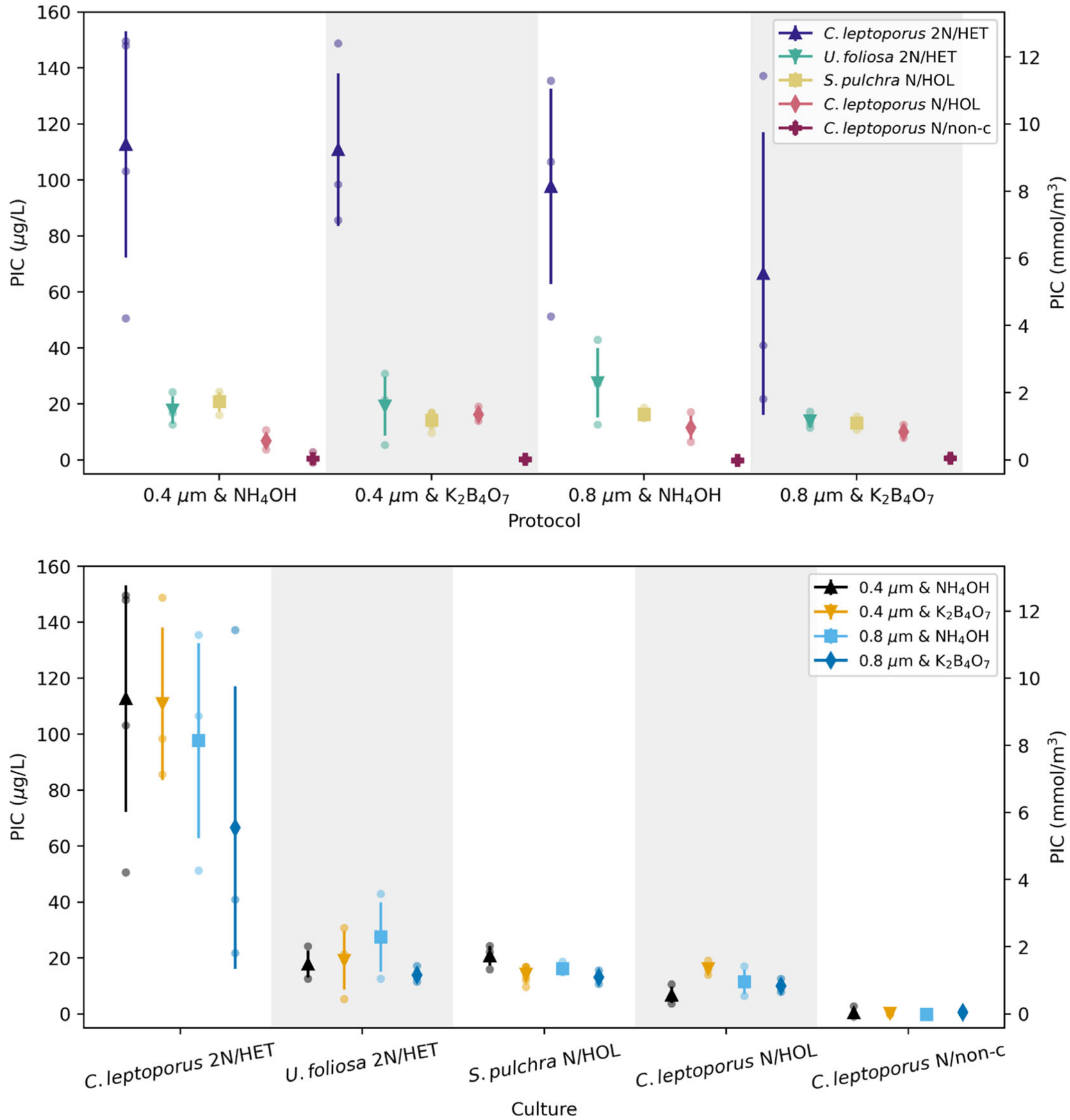

Fig. 2. Particulate inorganic carbon (PIC) for different culture strains and protocols. The dots represent each replicate, the solid symbols are the mean value for a given culture/protocol combination, and the lines are the standard deviation for a given culture/protocol combination.

Table 3. Basic statistics across the five strains.

	μg L^{-1}				mmol m^{-3}			
Code	**Avg**	**SD**	**Min**	**Max**	**Avg**	**SD**	**Min**	**Max**
C. leptoporus 2N/HET	98.23	45.12	21.72	149.60	8.19	3.76	1.81	12.47
C. leptoporus N/HOL	11.20	4.69	3.74	19.01	0.93	0.39	0.31	1.58
C. leptoporus N/non-c	0.29	0.92	−1.04	2.76	0.02	0.08	−0.09	0.23
U. foliosa 2N/HET	19.65	10.33	5.40	42.95	1.64	0.86	0.45	3.58
S. pulchra N/HOL	15.22	3.48	9.66	22.21	1.27	0.29	0.81	1.85

be zero. However, the measured PIC values for the *C. leptoporus* N/non-c culture were not exactly zero, with both positive and negative PIC values. The blank values for PIC were of a similar (and often larger) magnitude than the measured PIC concentration of the *C. leptoporus* N/non-c culture, resulting in some negative PIC values once the blank subtraction was performed (see

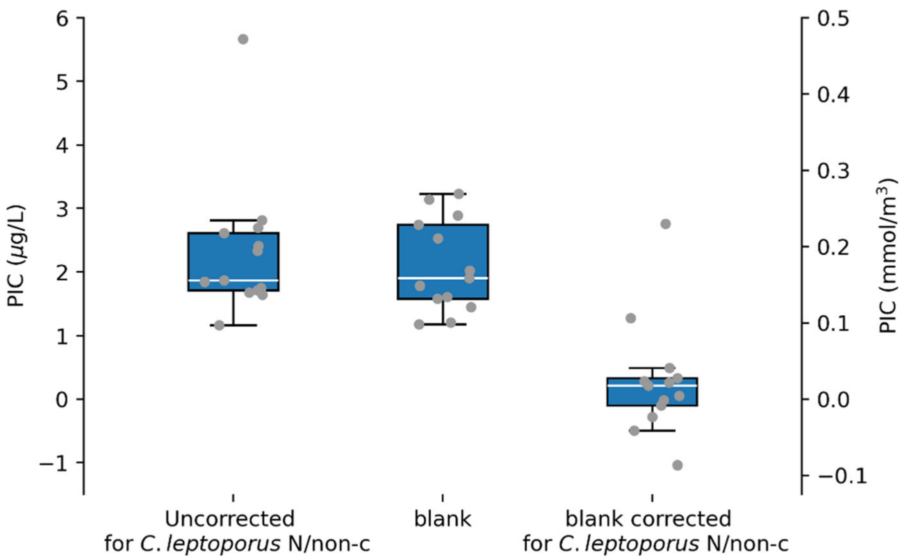

Fig. 3. Particulate inorganic carbon (PIC) for *C. leptoporus* N/non-c culture (blank corrected and not blank corrected) and for the blanks. The dots are each replicate from all the sampling protocols. The boxplots summarize these measurements, with the white line representing the median, the edges of the box representing the 25th and 75th percentiles and the whiskers extending to the farthest data point lying within 1.5 times the interquartile range from the box.

Table 4. Statistics on the *C. leptoporus* N/non-c culture.

C. leptoporus N/non-c	PIC (μg L^{-1})	PIC (mmol m^{-3})
Mean	0.073	0.006
Median	0.131	0.011
Standard deviation	0.288	0.024
Standard error	0.029	0.002
Median absolute deviation	0.175	0.015
Mean absolute deviation	0.241	0.020
Bias	0.000	0.000

Fig. 3). However, the blank subtraction results in a distribution of PIC concentration for the *C. leptoporus* N/non-c culture centered around zero. In the following analysis, we removed outliers based on the boxplot (Fig. 3).

To determine whether the PIC concentration for *C. leptoporus* N/non-c was statistically significant, we performed a one-sample *t*-test on the mean PIC value from the remaining *C. leptoporus* N/non-c data points with the null hypothesis that the mean is zero. The resulting *p* value was 0.28, indicating that we cannot reject the null hypothesis and that the mean is not significantly different from zero.

Similarly, a Wilcoxon test was conducted on the median PIC values with the null hypothesis that the median is zero. The *p* value obtained was 0.34, again suggesting that we cannot reject the null hypothesis and that the median is not significantly different from zero.

Detailed statistics on *C. leptoporus* N/non-c are provided in Table 4, showing that the mean and median PIC concentrations were close to zero. The standard deviation was 0.288 μg L^{-1} (0.024 mmol m^{-3}), and the standard error was 0.029 μg L^{-1} (0.002 mmol m^{-3}), indicating that while the mean and median were not significantly different from zero, there was still some variability in the measurements. The bias was calculated to be 0.000, suggesting no systematic error in the measurements. These statistical analyses reinforce that the measured PIC concentrations for the non-calcifying culture are not significantly different from zero, supporting the reliability and precision of our PIC measurement method. However, the variability in these measurements provides information on the precision of the full sampling procedure (from sample collection to analysis) and enables us to quantify the uncertainty in this discrete PIC sampling technique.

Discussion

Our study shows that PIC concentration is independent of the filter pore size and rinsing agent used. By using both the Kruskal–Wallis test and Aligned Rank Transform (i.e., one-way and two-way non-parametric tests), we concluded that any combination of the tested filter types and rinsing agents leads to statistically indistinguishable results. Further, by considering the non-calcifying culture, we demonstrated the precision of the sampling method and the different protocols: the mean and median PIC concentration were not statistically different from zero. This comprehensive evaluation confirms that the choice of filter types and rinsing agents during sampling has no significant effect on the precision or reliability of PIC measurements. Therefore, researchers have the flexibility to choose from different protocols without compromising data quality. By confirming that different sampling methods yield

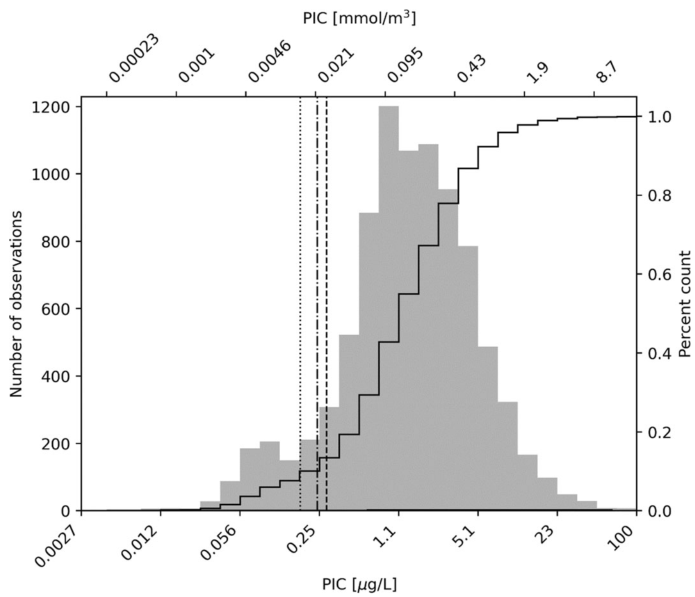

Fig. 4. Global PIC measurement values. The histogram shows the number of observations at each PIC concentration (left *y*-axis), with the solid line showing the cumulative distribution as a percentage of the total number of observations (right *y*-axis). The dashed line is the standard deviation, the dash-dot line is the mean absolute deviation, and the dotted line is the median absolute deviation; and the % of data below each line is: 10.8% for the standard deviation, 8.7% for the median absolute deviation, and 10.2% for the mean absolute deviation.

consistent PIC concentrations, our study simplifies methodological considerations and improves the comparability of data between studies and sites. This will contribute to a more comprehensive understanding of global PIC dynamics and will enable a more precise assessment of ocean carbon cycling and its impact on climate regulation.

The most important aspect of our study is the comprehensive assessment of measurement uncertainty associated with PIC sampling and analysis. By quantifying this uncertainty, we provide a solid foundation for the assessment of PIC data that allows researchers to distinguish between true variations in PIC concentrations and those that fall within the expected range of measurement error. This quantification further increases the reliability and comparability of PIC measurements between different studies and methods. The variability of our results shown in Table 4 reflects the precision of the method expressed in absolute numbers for different uncertainty metrics. Thus, a PIC concentration value below a given metric suggests that the value is beyond the detection limit and could reflect inherent limitations of the measurement procedure. However, PIC values larger than a given uncertainty metric can be considered significantly different from zero, indicating true PIC occurrences rather than artifacts of measurement variability or methodological error.

The inclusion of our uncertainty estimates may affect the interpretation of previous studies, especially at low PIC concentrations where the measurement uncertainty is significant relative to the measured values. In Fig. 4 we show the distribution of PIC measurements collected across the globe (data are from Mitchell et al. 2017, plus several more recent, unpublished cruises in the New England continental shelf, and the southern Pacific and Indian oceans). In general, 9–11% of the data fall below each uncertainty metric, highlighting the proportion of measurements affected by uncertainty and emphasizing the importance of precisely quantifying uncertainty in PIC measurements.

While we cannot say that the conclusions of previous studies need to be changed or are incorrect, any synthesis studies that rely on the very low PIC values may be affected by the uncertainties at those PIC concentrations. Therefore, moving forward, we suggest that data below a certain threshold (depending on your choice uncertainty metric) should be considered, but with appropriate error bars so that a rigorous error propagation can be included. The quantification and inclusion of uncertainties in the development of algorithms is essential to ensure confidence in satellite-based estimates over the full range of PIC values. The inclusion of uncertainties is critical for improving the robustness and precision of PIC estimates on the global scale.

In summary, the standardization of uncertainty assessments in PIC studies increases the reliability and comparability of measurements and allows researchers to precisely monitor and understand PIC dynamics. This contributes to a better understanding of ocean carbon cycles and their role in global climate regulation.

Acknowledgments

We acknowledge the efforts of William Balch, Dave Drapeau, and Bruce Bowler in collecting an expansive global dataset of discrete PIC measurements; Sunny Pinkham for collating and managing the global discrete PIC dataset; Farley Miller for coordinating the analysis of our experimental samples; and Michael Handley and the ICP-MS Facility at the Climate Change Institute, University of Maine, for processing the experimental samples. We also acknowledge valuable conversations with Dave Drapeau on PIC discrete sampling protocols. Mitchell would like to acknowledge funding from NASA to support her contributions to this work (80NSSC22K0197, 80NSSC21K1748), while Godrijan would like to acknowledge the EMBO Installation Grant (EMBO IG 5298-2023) and the European Union's NextGenerationEU program. Open access publishing facilitated by $WOA_OO_ELIGIBLE_INSTITUTION, as part of the Wiley - National and University Library in Zagreb Consortium Croatian Academic and Research Libraries Consortium agreement.

Conflicts of Interest

None declared.

References

Balch, W., and D. Drapeau. 2003. "Backscattering by Coccolithophorids and Coccoliths: Sample Preparation, Measurement and Analysis Protocols." In Ocean Optics Protocols for Satellite Ocean Color Sensor Validation, edited by J. L. Mueller, G. S. Fargion, and C. R. McClain, 27–36. Maryland: National Aeronautical and Space Administration.

Balch, W., and V. Fabry. 2008. "Ocean Acidification: Documenting its Impact on Calcifying Phytoplankton at Basin Scales." *Marine Ecology-Progress Series* 373: 239–247. https://doi.org/10.3354/meps07801.

Balch, W. M., D. T. Drapeau, T. L. Cucci, R. D. Vaillancourt, K. A. Kilpatrick, and J. J. Fritz. 1999. "Optical Backscattering by Calcifying Algae: Separating the Contribution of Particulate Inorganic and Organic Carbon Fractions." *Journal of Geophysical Research: Oceans* 104: 1541–1558. https://doi.org/10.1029/1998JC900035.

Balch, W. M., D. T. Drapeau, and J. J. Fritz. 2000. "Monsoonal Forcing of Calcification in the Arabian Sea." *Deep-Sea Research Part II: Topical Studies in Oceanography* 47: 1301–1337. https://doi.org/10.1016/S0967-0645(99)00145-9

Balch, W. M., H. R. Gordon, B. C. Bowler, D. T. Drapeau, and E. S. Booth. 2005. "Calcium Carbonate Measurements in the Surface Global Ocean Based on Moderate-Resolution Imaging Spectroradiometer Data." *Journal of Geophysical Research: Oceans* 110: C07001. https://doi.org/10.1029/2004JC002560.

Balch, W. M., P. M. Holligan, S. G. Ackleson, and K. J. Voss. 1991. "Biological and Optical Properties of Mesoscale Coccolithophore Blooms in the Gulf of Maine." *Limnology and Oceanography* 36: 629–643. https://doi.org/10.4319/lo.1991.36.4.0629.

Balch, W. M., and C. Mitchell. 2023. "Remote Sensing Algorithms for Particulate Inorganic Carbon (PIC) and the Global Cycle of PIC." *Earth-Science Reviews* 239: 104363. https://doi.org/10.1016/j.earscirev.2023.104363.

Balch, W. M., et al. 2014. "Surface Biological, Chemical, and Optical Properties of the Patagonian Shelf Coccolithophore Bloom, the Brightest Waters of the Great Calcite Belt." *Limnology and Oceanography* 59: 1715–1732. https://doi.org/10.4319/lo.2014.59.5.1715.

Ben-Joseph, O., et al. 2023. "Crystallization of Coccolith Calcite at Different Life-Cycle Phases Exhibits Distinct Degrees of Cellular Confinement." *Small Structures* 4: 2200353. https://doi.org/10.1002/sstr.202200353.

Billard, C., and I. Inouye. 2004. "What Is New in Coccolithophore Biology?" In Coccolithophores: From Molecular Processes to Global Impact, edited by H. R. Thierstein and J. R. Young, 1–29. Berlin: Springer Berlin Heidelberg.

Bishop, J. K. B., et al. 2022. "Transmitted Cross-Polarized Light Detection of Particulate Inorganic Carbon Concentrations and Fluxes in the Ocean Water Column: Ships to ARGO Floats." *Frontiers in Remote Sensing* 3: 837938. https://doi.org/10.3389/frsen.2022.837938.

Brownlee, C., G. Langer, and G. L. Wheeler. 2021. "Coccolithophore Calcification: Changing Paradigms in Changing Oceans." *Acta Biomaterialia* 120: 4–11. https://doi.org/10.1016/j.actbio.2020.07.050.

Daniels, C. J., T. Tyrrell, A. J. Poulton, and L. Pettit. 2012. "The Influence of Lithogenic Material on Particulate Inorganic Carbon Measurements of Coccolithophores in the Bay of Biscay." *Limnology and Oceanography* 57: 145–153. https://doi.org/10.4319/lo.2012.57.1.0145.

Daniels, C. J., et al. 2018. "A Global Compilation of Coccolithophore Calcification Rates." *Earth System Science Data* 10: 1859–1876. https://doi.org/10.5194/essd-10-1859-2018.

Fernández, E., P. Boyd, P. M. Holligan, and D. S. Harbour. 1993. "Production of Organic and Inorganic Carbon within a Large Scale Coccolithophore Bloom in the North Atlantic Ocean." *Marine Ecology Progress Series* 97: 271. https://doi.org/10.3354/meps097271.

Frada, M., E. M. Bendif, S. Keuter, and I. Probert. 2019. "The Private Life of Coccolithophores." *Perspectives in Phycology* 6: 11–30. https://doi.org/10.1127/pip/2018/0083.

Gordon, H. R., G. C. Boynton, W. M. Balch, S. B. Groom, D. S. Harbour, and T. J. Smyth. 2001. "Retrieval of Coccolithophore Calcite Concentration from SeaWiFS Imagery." *Geophysical Research Letters* 28: 1587–1590. https://doi.org/10.1029/2000GL012025.

Gorman, E., et al. 2019. The NASA Plankton, Aerosol, Cloud, Ocean Ecosystem (PACE) Mission: An Emerging Era of Global, Hyperspectral Earth System Remote Sensing. France: SPIE.

Henriksen, K., S. L. S. Stipp, J. R. Young, and M. E. Marsh. 2004. "Biological Control on Calcite Crystallization: AFM Investigation of Coccolith Polysaccharide Function." *American Mineralogist* 89: 1709–1716. https://doi.org/10.2138/am-2004-11-1217

Holligan, P. M., et al. 1993. "A Biogeochemical Study of the Coccolithophore, *Emiliania huxleyi*, in the North Atlantic." *Global Biogeochemical Cycles* 7: 879–900. https://doi.org/10.1029/93GB01731.

Honjo, S., R. Francois, S. Manganini, J. Dymond, and R. Collier. 2000. "Particle Fluxes to the Interior of the Southern Ocean in the Western Pacific Sector along 170°W." *Deep-Sea Research Part II: Topical Studies in Oceanography* 47: 3521–3548. https://doi.org/10.1016/S0967-0645(00)00077-1.

Hopkins, J., and W. M. Balch. 2018. "A New Approach to Estimating Coccolithophore Calcification Rates from Space." *Journal of Geophysical Research: Biogeosciences* 123: 1447–1459. https://doi.org/10.1002/2017JG004235.

Klaas, C., and D. E. Archer. 2002. "Association of Sinking Organic Matter with Various Types of Mineral Ballast in the Deep Sea: Implications for the Rain Ratio." *Global*

Biogeochemical Cycles 16: 63-61–63-14. https://doi.org/10.1029/2001GB001765
Knecht, N. S., et al. 2023. "The Impact of Zooplankton Calcifiers on the Marine Carbon Cycle." *Global Biogeochemical Cycles* 37: e2022GB007685. https://doi.org/10.1029/2022GB007685.
Langer, G., et al. 2021. "Role of Silicon in the Development of Complex Crystal Shapes in Coccolithophores." *The New Phytologist* 231: 1845–1857. https://doi.org/10.1111/nph.17230.
Mayers, K. M. J., et al. 2019. "Growth and Mortality of Coccolithophores during Spring in a Temperate Shelf Sea (Celtic Sea, April 2015)." *Progress in Oceanography* 177: 101928. https://doi.org/10.1016/j.pocean.2018.02.024
Millero, F. 2013. "Composition of the Major Components of Seawater." In Chemical Oceanography, 4th ed. Boca raton: CRC Press.
Millero, F. J. 2007. "The Marine Inorganic Carbon Cycle." *Chemical Reviews* 107: 308–341. https://doi.org/10.1021/cr0503557.
Milliman, J. D. 1993. "Production and Accumulation of Calcium Carbonate in the Ocean: Budget of a Nonsteady State." *Global Biogeochemical Cycles* 7: 927–957. https://doi.org/10.1029/93GB02524.
Mitchell, C., C. Hu, B. Bowler, D. Drapeau, and W. M. Balch. 2017. "Estimating Particulate Inorganic Carbon Concentrations of the Global Ocean from Ocean Color Measurements Using a Reflectance Difference Approach." *Journal of Geophysical Research: Oceans* 122: 8707–8720. https://doi.org/10.1002/2017JC013146.
Monteiro, F. M., et al. 2016. "Why Marine Phytoplankton Calcify." *Science Advances* 2: e1501822. https://doi.org/10.1126/sciadv.1501822.
Moore, T. S., M. D. Dowell, and B. A. Franz. 2012. "Detection of Coccolithophore Blooms in Ocean Color Satellite Imagery: A Generalized Approach for Use with Multiple Sensors." *Remote Sensing of Environment* 117: 249–263. https://doi.org/10.1016/j.rse.2011.10.001.
Neukermans, G., L. T. Bach, A. Butterley, Q. Sun, H. Claustre, and G. R. Fournier. 2023. "Quantitative and Mechanistic Understanding of the Open Ocean Carbonate Pump—Perspectives for Remote Sensing and Autonomous In Situ Observation." *Earth-Science Reviews* 239: 104359. https://doi.org/10.1016/j.earscirev.2023.104359.
Platzner, T. I., I. Segal, and L. Halicz. 2008. "Selected isotope ratio measurements of light metallic elements (Li, Mg, Ca, and Cu) by multiple collector ICP-MS." *Anal Bioanal Chem* 390: 441–450. https://doi.org/10.1007/s00216-007-1668-2
Poulton, A. J., et al. 2006. "Phytoplankton Mineralization in the Tropical and Subtropical Atlantic Ocean." *Global Biogeochemical Cycles* 20: GB4002. https://doi.org/10.1029/2006GB002712.
Van Iperen, J., and W. Helder. 1985. "A Method for the Determination of Organic Carbon in Calcareous Marine Sediments." *Marine Geology* 64: 179–187. https://doi.org/10.1016/0025-3227(85)90167-7.
Winter, A., and W. G. Siesser. 1994. Coccolithophores. Cambridge: Cambridge University Press.
Young, J. R., et al. 2003. "A Guide to Extant Coccolithophore Taxonomy." *Journal of Nannoplankton Research* 1: 124. https://doi.org/10.58998/jnr2297
Ziveri, P., et al. 2023. "Pelagic Calcium Carbonate Production and Shallow Dissolution in the North Pacific Ocean." *Nature Communications* 14: 805. https://doi.org/10.1038/s41467-023-36177-w

Submitted 04 October 2024
Revised 28 February 2025
Accepted 05 March 2025